FINAL CONTRACT REPORT

EVALUATION OF THE IN-SERVICE PERFORMANCE OF THE TOM'S CREEK BRIDGE FIBER-REINFORCED POLYMER SUPERSTRUCTURE

W. D. Neely and T. E. Cousins
Via Department of Civil and Environmental Engineering

S. P. Phifer, J. L. Senne, S. W. Case, and J. J. Lesko
Department of Engineering Science and Mechanics

Virginia Polytechnic Institute and State University

Project Manager
Jose Gomez, Ph.D., P.E., Virginia Transportation Research Council

Contract Research Sponsored by the
Virginia Transportation Research Council

Virginia Transportation Research Council
(A Cooperative Organization Sponsored Jointly by the
Virginia Department of Transportation and
the University of Virginia)

Charlottesville, Virginia

September 2003
VTRC 04-CR5

NOTICE

The project that is the subject of this report was done under contract for the Virginia Department of Transportation, Virginia Transportation Research Council. The contents of this report reflect the views of the authors, who are responsible for the facts and the accuracy of the data presented herein. The contents do not necessarily reflect the official views or policies of the Virginia Department of Transportation, the Commonwealth Transportation Board, or the Federal Highway Administration. This report does not constitute a standard, specification, or regulation.

Each contract report is peer reviewed and accepted for publication by Research Council staff with expertise in related technical areas. Final editing and proofreading of the report are performed by the contractor.

ABSTRACT

The Tom's Creek Bridge is a small-scale demonstration project involving the use of fiber-reinforced polymer (FRP) composite girders as the main load carrying members. It is a simply supported, short-span bridge located along Tom's Creek Road in Blacksburg, Virginia. As a result of discussions among Virginia Tech, Strongwell, the Virginia Department of Transportation, and the Town of Blacksburg, the existing deteriorated superstructure of the Tom's Creek Bridge was replaced with a glue-laminated timber deck on 8 in (20.3 cm) deep pultruded fiber-reinforced polymer beams.

The project was intended to address two issues. First, by calculating bridge design parameters such as the dynamic load allowance, transverse wheel load distribution and deflections under service loading, the Tom's Creek Bridge will aid in modifying current AASHTO bridge design standards for use with FRP composite materials. Second, by evaluating the FRP girders after being exposed to controlled laboratory and service conditions, the project will begin to answer questions about the long-term performance of these advanced composite material beams when used in bridge design.

A dynamic load allowance, IM, of 0.90 is recommended for the Tom's Creek Bridge. This value is the largest average IM observed and is therefore conservative. This value is significantly higher than those set forth in the AASHTO standards of 0.33 (AASHTO, 1998) and 0.30 (AASHTO, 1996). It is recommended to use a value of L/425 (LRFD Specification) or L/500 (Standard Specification). This value is consistent with AASHTO deflection control criteria for an all timber bridge. It is recommended to use the AASHTO wheel load distribution factors for a glulam timber deck on steel stringer bridge. There is no indication of loss of FRP girder ultimate strength after 15 months of service. Given the low service loads (no more than 10% of the ultimate capacity) and traffic volume the fatigue life prediction model suggests that fatigue will not be a major concern during the life of service (10 to 15 years).

INTRODUCTION

If FRP composite materials are to be routinely used in future bridge engineering a priority must be placed on determining how these new material systems behave in-service. Examining these composites material components under both controlled laboratory and field conditions is critical to developing a design specification and establishing confidence in fiber-reinforced polymer composites within the bridge design and construction community. The laboratory and field work undertaken as part of the Tom's Creek Bridge installation in Blacksburg, Virginia serves as an opportunity to gain valuable insight into the structural and long-term performance of the double web beam (DWB) fabricated by Strongwell, Corp.

The Tom's Creek Bridge is a small-scale demonstration project involving the use of fiber-reinforced polymer (FRP) composite girders as the main load carrying members. The project is intended to address two issues. First, by calculating bridge design parameters such as the dynamic load allowance, transverse wheel load distribution and deflections under service loading, the Tom's Creek Bridge will aid in modifying current AASHTO bridge design standards for use with FRP composite materials. Second, by evaluating the FRP girders after being exposed to controlled laboratory and service conditions, to begin to answer questions about the long-term performance of these advanced composite material beams when used in bridge design.

The Tom's Creek Bridge is a simply supported, short-span bridge located along Tom's Creek Road in Blacksburg, Virginia. Owned by the Town of Blacksburg, the bridge was originally constructed in 1932 and then rebuilt in 1964. The rebuilt bridge spanned 17.5 ft (5.33 m) and was 24 ft (7.32 m) wide. The bridge superstructure consisted of twelve W10 x 21 stringers; each 20 ft (6.10 m) in length while the substructure was composed of two concrete abutments. The deck system utilized 4 in. x 8 in. (10.2 cm x 20.3 cm) transverse timber plank flooring with a 2 to 3 in. (5 to 8 cm) asphalt overlay. The original structure had a load rating of 20 tons (178 kN), however, a bridge inspection in 1990 discovered significant corrosion in a number of the stringers and as a result the bridge's rating was reduced to 10 tons (89.0 kN). At that time Tom's Creek Road was planned for widening in 10-15 years. As a result, the Town of Blacksburg was interested in a temporary repair solution for the bridge's structural deficiencies. As a result of discussions between Virginia Tech, Strongwell, the Virginia Department of Transportation, and the Town of Blacksburg, the existing deteriorated superstructure of the Tom's Creek Bridge was replaced with a glue-laminated timber deck on 8 in (20.3 cm) deep pultruded fiber-reinforced polymer beams.

Prior to the bridge's rehabilitation in the summer of 1997, the new bridge's superstructure was constructed and tested at the Structures and Materials Research Laboratory at Virginia Tech. Once constructed, the bridge was field tested by Virginia Tech and VTRC. Detailed information on the design of the Tom's Creek Bridge, as well as the laboratory and initial field testing program may be found in work by Hayes et al. (Hayes, 1998; Hayes, 2000). At the time of construction, the Tom's Creek Bridge was scheduled for five load tests. These tests occurred in six-month intervals for the first two years of the bridge's service life. This regular testing made it possible to assess the bridge's response to vehicular loading initially and as a function of time. In addition, the bridge had a unique design that enabled researchers at Virginia Tech to extract two beams in September of 1998, after fifteen months of service, and test these beams for any losses in both strength and stiffness.

The fiber-reinforced polymer composite beams used in the Tom's Creek Bridge superstructure were manufactured using the pultrusion method. The pultrusion process involves the pulling of reinforcing fibers and resin matrix through a die, or series of dies, that shape and cure the material (Hyer, 1998). The FRP composite beam (Figure 1) is composed of glass and carbon fibers in a vinyl ester matrix. During the pultrusion process 10% styrene by weight and some additional filler are typically added. Although the beams do not contain any ultraviolet (UV) inhibitors, the carbon black filler provides some protection against UV radiation. Continuous strand mat, glass roving, $0/90^{\circ}$ and $\pm 45^{\circ}$ fabric are used throughout the section while carbon fiber tows are dispersed within the flanges to supply increased flexural stiffness. The FRP composite beams were manufactured in two batches and then shipped to Virginia Tech. The targeted fiber (both E-glass and carbon) volume fraction for the beam is 55% by weight. The web and flange sections are essentially quasi-isotropic with the flanges also containing carbon fiber laminae. The double-web design of the beam provides an increase in shear resistance as well as buckling and torsion resistance. Further details of the make-up and use of the double web beam can be found in a design guide published by Strongwell Corporation.(Strongwell, 2000). There are twenty-four of the FRP composite beams utilized in the Tom's Creek Bridge. The beams measure 20 ft (6.10 m) in length and weigh 11.2 lb/ft (163 N/m). Section properties for the composite girders are given in Table 1. Individual girder locations and modulus of elasticity values can be found in Hayes (1998).

The Tom's Creek Bridge rehabilitation used the preexisting concrete abutments, therefore maintaining the same 17.5 ft (5.33 m) span and 12.5 in skew as the original bridge. The girders were secured to the concrete abutments using pressure treated 2 x 4 sections, threaded rods and anchor bolts. The threaded rods were anchored into pre-drilled holes in the abutments using epoxy cement. The girders are sandwiched between the abutment and the 2 x 4 sections through the use of anchor bolts that screw into the threaded rods. The glue-laminated deck structure for the FRP composite Tom's Creek Bridge consists of seven 24.5 ft x 2.83 ft x 0.427 ft (7.47 m x 0.86 m x 0.13 m) sections placed transversely across the bridge. The deck was fastened to the composite girders using through bolts and pressure treated 2 x 4 sections at 323 locations. Through the use of steel angles and curb rails the new bridge rail is connected directly to the glue-laminated deck. A detailed description of the Tom's Creek Bridge composite deck-to-girder connections may be found in the theses of Neely (2000) and Hayes (1998).

There were two purposes for connecting the timber deck to the FRP composite girders: to resist uplift forces from the vehicular traffic and to attempt to provide additional superstructure stiffness through partial composite action. The partial composite action would allow the bridge's glue-laminated deck and FRP composite girders to act together to resist applied load. As a result, the bridge would experience an increase in stiffness. The wearing surface of the Tom's Creek Bridge consists of a 4.5 in (114 mm) asphalt base course and a 1.5 in (38 mm) surface course. A water proofing membrane separates the base course and surface course. The Tom's Creek Bridge was completed on June 27, 1997, after only 4 days of construction (Figure 2).

PURPOSE AND SCOPE

The purpose of the research reported in this paper is to investigate how the fiber-reinforced polymeric composite girders used in the Tom's Creek Bridge superstructure behave under actual service loading conditions. This is further broken down into the following areas:

1. Stiffness of the FRP composite bridge
2. FRP girder's performance with respect to AASHTO bridge design parameters
3. In-service and laboratory fatigue performance of the hybrid FRP composite beams
4. Development of an initial life prediction scheme for the FRP girder

This information may then be used in conjunction with other FRP composite demonstration projects to assist in modifying current AASHTO Specifications for bridge design.

METHODS

Data from five load tests performed on the Tom's Creek Bridge were analyzed. Service strains and deflections were studied to determine if the stiffness of the FRP composite bridge change with time. Also, tightening of the deck-to-girder connections was evaluated to determine how this variable affected the bridge's stiffness. The dynamic load allowance (IM) and girder distribution factors (g) were determined. These performance parameters offered insight into the bridge's performance and allowed for comparisons with AASHTO bridge design requirements. Finally, the long-term performance of the fiber-reinforced polymeric composite girders was investigated. Strength and stiffness tests were performed on two FRP composite girders that were removed from the composite bridge after fifteen months of service. The stiffness data were compared to data from those same girders obtained during stiffness tests conducted prior to the construction of the Tom's Creek Bridge. Strength data obtained from failing the removed girders were compared to beams that were failed from the same batch prior to construction.

Field Testing

The Tom's Creek Bridge was instrumented with both strain gages and deflectometers to record the bridge's behavior during load testing. In order to depict a clear picture of the bridge's performance, the number and location of these devices evolved during the first three load tests. After the third load test, in the fall of 1998, the final instrumentation plan was established. This instrumentation plan was used for the spring of 1999 and fall of 1999 load tests. The initial and final instrumentation plans are presented in Figure 3.

Instrumentation

The Tom's Creek Bridge was instrumented with strain gages to measure the surface strains of the FRP composite girders during the testing. The flexural performance of the bridge was monitored using both bottom (B) and top (T) flange gages located at mid-span of the FRP composite girders. Top flange bending was measured on girders 2 and 12 while the location of bottom flange strain gages varied (Figure 3). Axial behavior of the bridge girders was monitored on girders 2 and 12. The axial data were measured using strain gages (A) attached to the girder's

web 24 in from the southern abutment. In addition, top flange gages and axial web gages were positioned in pairs of two. One gage was located on the upstream side of the girder while the other gage was placed symmetrically on the downstream side of the girder. This allowed for any torsional behavior of the bridge girders to be recorded.

Data from the Tom's Creek Bridge load tests were collected using a high-speed data acquisition system. The system was configured to sample at a rate of 200 scans per second per channel for each load test. All of the electrical equipment was kept inside a van for the duration of the test and was powered by a portable AC generator.

Controlled Vehicle

The VDOT truck used for load testing was a three-axle dump truck that was loaded with gravel from a nearby rock quarry. The average truck weight for the Tom's Creek Bridge field tests was 48.8 kips (217 kN) when filled with gravel. The three-axle VDOT dump truck was determined to carry approximately 30% of the vehicle weight with the front axle and 70% with the rear two axles or tandem. The axle weights were based on the ratio of maximum deflection data as the front and rear axles cross the bridge and were consistent with weight distributions used in other studies on the dynamic analysis of bridges (Hwang, 1990). The axle weights of the VDOT truck were slightly in excess of the Virginia legal limit for a three-axle dump truck.

Field Test Procedure and Analysis

The Tom's Creek Bridge was tested on five occasions: fall 1997, spring 1998, fall 1998, spring 1999, and fall of 1999. Fall tests were typically done in mid-October while spring tests were typically done in mid-May. A timeline that details the history of the Tom's Creek Bridge, including the above-mentioned field tests is shown in Figure 4. For all of the load tests the truck passed over the bridge in three different locations. It made a right lane pass, a left lane pass or a center lane pass. For all references in this report the right lane refers to the upstream side of the bridge and the left lane refers to the downstream side of the bridge. All right lane passes had the truck heading north while left lane passes had the truck heading south. Center lane passes were conducted with the truck going either north or south. The truck passed over the bridge at three different speeds. For a quasi-static condition the truck would idle over the bridge at a speed of approximately 2 mph (3.2 km/h).

To investigate the ability of the deck-to-girder connections to provide partial composite action additional load tests of the bridge were conducted immediately after all the connections were tightened. All other load tests discussed in this paper were conducted with the connections unaltered (as found on the day of load testing) so that a true in-service evaluation of the bridge could be made. The service strains and deflections of the bridge before ("As Is") and after ("Tightened") the connections were tightened were compared to determine the increase in stiffness in the bridge super-structure that would result.

Dynamic load allowance (IM) is the increase of the static weight of a vehicle due to its movement across a bridge. The dynamic load allowance for the bridge was calculated using both strain and deflection measurements recorded during the field tests. To test the bridge's dynamic performance and thus determine the IM the test truck passed over the bridge at 25 mph (40 km/h)

and 40 mph (64 km/h). Forty miles per hour represents the maximum speed that the VDOT truck could safely cross the bridge. For each position (right, left, and center) on the bridge the truck usually crossed five times at each speed (idle, 25 mph and 40 mph). The one exception to this is the fall 1997 load test. This was the first load test and predominantly served as a trial to verify the test set-up and determine if more gages and/or deflectometers should be added. Therefore, only about two truck crossings at each position at each speed were conducted over the bridge. Quasi-static structural response was recorded when the VDOT dump truck idled across the bridge at approximately 2 mph (3.2 km/h). These data are referred to as "static" and was used as a baseline for all IM calculations.

The first step in calculating the dynamic load allowance for the Tom's Creek Bridge was to determine the average peak static response for each lane on the bridge. For each lane crossing, the measured peak response for all trucks crossings was determined. These values were then averaged to establish the average peak static strain, or deflection, per lane crossing.

The next step in determining the dynamic load allowance was to obtain the peak response for each truck crossing at both 25 and 40 mph (40 and 64 km/h). These data were separated out by lane and by speed. Next, these peak values were divided by the corresponding average peak static strain, or deflection, for that given lane to formulate the dynamic response. The IM is equal to this dynamic response minus one as shown by the following equation:

$$IM = \frac{R_{dyn}}{R_{stat}} - 1.0 \qquad (1)$$

where: IM = The dynamic load allowance

R_{dyn} = The peak dynamic response (strain or deflection) at 25 or 40 mph

R_{stat} = The average peak static response (strain or deflection) at 1 mph

Once the IM was calculated for all of the runs in a given lane, the results were averaged to determine the dynamic load allowance for that lane. This procedure was carried out for all five load tests at both 25 and 40 mph (40 and 64 km/h). A similar procedure was followed when determining the wheel load distribution factor for all five load tests.

In bridge design, the girder or transverse wheel load distribution factor (g) is typically used in design to calculate the design load for a specific girder in a slab-girder bridge. It is a function of span length and type of superstructure. Current AASHTO standards do not include g for this innovative structural system. The first step in calculating the transverse load distribution for the Tom's Creek Bridge was to locate the girder having the peak response for each truck crossing and determine the corresponding magnitude. After the peak response and girder number were determined, the time during the truck crossing at which this maximum value occurred was established. Next, the response values for all of other girders at that instant in time were noted in a tabular format. The result of this process was a "snapshot" of all the girder responses as the peak response in a single girder occurred. Then the sum of all of the individual strains or deflections was calculated and each individual girder response was divided by this total. The result was a fraction of the truck weight that each individual composite girder carried. The procedure for calculating the transverse wheel load distribution was the same, regardless of

whether the data originated from strain gages or deflectometers. The only difference lay in the number of measuring devices. The number and location of strain gages and deflectometers used during the load tests may be seen in Figure 3. Just as it was for determining the dynamic load allowance, linear interpolation was used to estimate the response for the composite girders that were not equipped with strain gages or deflectometers. The value of g was formulated based on the mid-span response of the FRP composite girders under heavy truck loading.

Laboratory Test Procedures and Analysis

Residual Girder Performance Assessment

In September of 1998 girders 1 and 2 were removed from the bridge and replaced with two new FRP composite girders. Removed girders were brought back to the Structures and Materials Research Laboratory at Virginia Tech where they were tested for stiffness and strength. These data were then compared to strength and stiffness data from tests conducted prior to the construction of the Tom's Creek Bridge. After 15 months of service two FRP composite girders were removed from the Tom's Creek Bridge and tested for stiffness and strength. The post-service stiffness and strength assessed was then compared to values obtained during lab testing of the composite beams prior to construction of the Tom's Creek Bridge (Hayes, 1998). For strength comparisons, data obtained from girders one and two were compared to the test results for beams from the same batch that were tested to failure prior to construction of the bridge and reported by Hayes (1998). Thus, a direct comparison was made for the purpose of determining any changes in the stiffness of the beams. These comparisons have been performed as an initial step in determining the long-term performance of FRP composite girders exposed to actual bridge service conditions and will be discussed.

The stiffness and strength test setup for beams one and two consisted of a four-point bending geometry laterally unsupported. The span length was 17.5 ft (5.33 m) and two equal point loads were applied to the composite girder one foot from either side of mid-span (Figure 5). This four-point bending geometry allowed for constant moment and zero shear at mid-span. Load was applied to the beam using a 200 kip (890 kN), 36 in. (914 mm) stroke, manual hydraulic actuator. The load was monitored using a 200 kip (890 kN) load cell. Deflections were recorded with wire potentiometers at the mid-span and quarter points of the beam. Bending strain gages were located on the top flange and bottom flange at mid-span, while shear strain gages were located at the quarter point and mid-span.

The beams were loaded to approximately 7.5 kips (33.4 kN) and then unloaded to assess stiffness. This loading-unloading cycle was repeated three times and the final stiffness value is the average stiffness obtained from the three loading cycles. After a beam was tested for stiffness, the beam was then loaded to failure so that the ultimate strength of the beam could be determined. To test the beams' ultimate strength, the beams were loaded in a similar manner to that of the stiffness tests. However, instead of stopping at 7.5 kips (33.4 kN), the application of the load on the FRP composite girder was continued until failure of the beam. All data were recorded using the same data acquisition system that was used for the Tom's Creek Bridge field tests.

Laboratory Assessment of Girder Fatigue Performance

Full-scale fatigue tests were run at a 14 ft (4.27 m) span, similar to the bridge. Four beams were examined to understand the fatigue response and associated failure mode.

The fatigue condition selected was a four-point bend test, loaded at 1/3 points. This test configuration was similar to the quasi-static tests and simplifies the analysis, due to the presence of a constant moment region. The test configuration can be seen in Figure 6.

The data collected from the test were predominately to monitor stiffness reduction throughout the test, and ensure there was no torsional loading of the beam. The data were collected using the MEGADAC 3108 data acquisition system, which allows for 200 scans/second/channel. Gage locations and types are shown in Figure 6.

The loads applied were based on the moment capacity found in the static tests. These loads were at approximately 9 times the actual loading the bridge beams would see in service at the Tom's Creek Bridge. The tests were run under load control, using an MTS controller. The R-ratio (min load/ max load) was desired to be 0.1. In reality, due to the large deflections, the capabilities of the pump controlled the load ratios and speed of the test; the maximum and minimum actuator loads and the frequencies are summarized in Table 2. These values were consistently held throughout the test. The table also compares the loading to the ultimate moment of the batch and also to the overall average ultimate moment.

Periodic quasi-static tests were completed on the beams and the strains and deflections listed above were collected. The load was applied under displacement control up to the maximum load of the respective test. From the data, stiffness values could be calculated and the influence of cyclic loading on the system was analyzed as outlined below.

Development of a Fatigue Life Prediction Scheme for the 8-Inch-Deep DWB

Methodology Assumptions

The durability of FRP sections and assemblies remains a major question in their use as primary load bearing members and structures. Moreover, how capacity and structural stiffness will change over time present a central conundrum for designers when specifying allowable loads and reductions factors. It is safe to say that the community cannot wait, nor does it possess the resources, to qualify all full-scale structural elements and systems under the many varied service environment conditions possible nationally. To allow for sufficiently generalized descriptions of life, credible simulations that accurately describe the combination of synergism of load and environment must be used to ensure practical and efficient design guidelines for durability. These simulations must be robust and be developed from reliable descriptions of material degradation mechanisms and their interactions, which may include characterizations from accelerated testing to extend the validity of the predictions. Such simulations must be validated over a wide range of conditions, at both the component and structural levels.

One must also recognize that the traditional linear cumulative damage theory (Miner's Rule) is not sufficient to describe FRP life. Given these circumstances take the following approach to assess the useful life of an FRP component or structure.

1. Establish how service life will be judged (e.g., loss of a certain percentage of stiffness, complete failure).
2. Identify the governing failure mode(s) (coined the critical element) and possible shifts in failure mode(s).
3. Assess the dominant stress state(s) that influence the failure mode(s).
4. Postulate that remaining strength of the controlling failure mode may be used as the damage metric.
5. Track residual stiffness of the FRP material that influences the stress state which controls the failure mode(s) of interest.

The culmination of these principles is embodied in a life prediction methodology based on remaining strength (Reifsnider et al., 1996). This methodology assumes that remaining strength may be determined (or predicted) as a function of load level (and environment) and some form of generalized time (i.e., cycles to failure in the case of fatigue). Keeping track of how the residual strength changes, the number of cycles to failure can be determined by comparing it to the stress which is it sees within the component. When the applied stress exceeds the residual strength the component fails and we call that life, N in the case of fatigue, as illustrated in Figure 7.

In the case of composites we use this concept of residual strength as a metric for assessing life, a failure mode is assumed. That failure mode which controls the life of the composite is called the critical element. As an example, consider a cross ply laminate with layers of fibers running in both the 0° and the 90° directions. If we consider a tensile load applied in the 0° direction, the first plies to fail in this cross ply composite are the 90° plies. Although the 90° plies "fail" (i.e., cracking in the 90° plies) the laminate has not failed. However, if a higher stress is applied to the cross ply laminate, high enough to fail the 0° plies, the laminate will then fail. For the cross ply laminate the failure mode of interest and the one we follow in terms of residual strength is the 0° ply. We call this ply the "critical element." The 90° plies are labeled the "sub-critical elements" as they do not cause the failure of the laminate, yet they do influence the stress applied to the critical element as shown in Figure 7. That is cracking in the 90° plies, or the sub-critical element results in a redistribution of stress from the 90°s to the 0° plies. This can be sensed by monitoring the change in stiffness.

Thus the goal of this analysis is to find ways to describe how these two quantities (stiffness and strength) change and keep track of them as a function of service. This is accomplished by accounting for all of the degradation mechanisms that reduce the stiffness and strength either through first principles or phenomenological means.

This method has been employed, with some validation, to assessing the fatigue life of a hybrid FRP shape (Senne, 2000a). Delamination within the hybridized region of the flange was shown to be the controlling failure mode in both quasi-static and fatigue loading (Figure 8) and is therefore considered the critical element. Consider the case where the DWB is subjected to four-point bending fatigue loading. The remaining strength approach is employed for the analysis of life of this girder. The model employs the idea that initially stiffness reduction only occurs in the tensile flange. As the stiffness of the bottom/tensile flange is reduced, there is a redistribution of strain to the compressive flange and an inherent shift in the neutral axis. The remaining

strength approach, in conjunction an iterative stress analysis is then used to determine the onset of delamination and the crack growth to failure. The assumptions employed in the residual strength model include:

- Reduction in tensile stiffness of the beam will be evaluated, based on tensile coupon data of similar material conducted by Phifer (1999,) which focuses on off-axis plies.
- The unidirectional carbon plies do not experience any stiffness reduction.
- Strength reduction is uniform for both the tensile and compression flanges and is related to the in-plane strength reduction of the tensile flange.
- The carbon acts stiffer in tension than in compression, therefore the neutral axis is initially offset toward the tensile flange but during loading shifts toward the compressive side.
- The tensile out-of-plane strength (Z_t) is calculated from the Mult found from quasi-static failure testing.
- Once delamination initiates, stiffness reduction must be accounted for in the compression flange in addition to the tensile flange.
- Crack growth, once delamination is initiated, is symmetric from each side of the beam, across the width of the beam (in the y-direction).
- Failure occurs when the crack propagates across the width of the beam or if the in-plane remaining strength matches the loading.

The flowchart in Figure 9 graphically describes the process required to assess life. The process begins by inputting the geometry, layup (orientation of plies within the laminate) and loading. Using this information the stresses and strains are evaluated. The free edge stresses are then compared to the strength of the top flange. If the stress exceeds the in-plane strength, delamination is assumed. If the stress does not exceed the strength, the stiffness in the tensile flange is reduced based on a maximum strain criterion. The neutral axis shift corresponding to the stiffness reduction is then calculated. The new stiffness and neutral axis location are used in Laminated Beam Theory to determine the new EI_{eff} and curvature. The κ_x^0 (the mid-plane bending curvature of the beam) becomes the new loading condition for the stress evaluation. The process is continued until delamination initiation. After delamination has initiated, the growth of the delamination is tracked until it has reached the full width of the flange. As the delamination grows, the reduction of the top flange stiffness is calculated by considering the generation of the two sublaminates. The details of the delmination initiation and propagation are discussed below. Further details on this analysis are discussed in Senne (2000a & b).

Out-of-Plane Strength Properties

The out of plane strength controls the fatigue performance of the girder. By employing the quadratic delamination failure criteria proposed by Brewer and Lagace (1988) delamination initiation is predicted based on the out-of-plane stresses and strengths. Failure occurs when,

$$\left(\frac{\tau_{xz}}{Z_{xz}}\right)^2 + \left(\frac{\sigma_z}{Z_t}\right)^2 \geq 1 \qquad (2)$$

where τ_{xz} and σ_z are the out of plane interlaminar stresses at a point in the laminate and are compared to the respective out of plane strengths Z_{xz} and Z_z. In term of a failure criterion, Equation (2) may be expressed as

$$Fa_{out-of-plane} = \sqrt{\left(\frac{\tau_{xz}}{Z_{xz}}\right)^2 + \left(\frac{\sigma_z}{Z_t}\right)^2} \qquad (3)$$

where the out of plane applied stresses $Fa_{out\text{-}of\text{-}plane}$ are compared to the quadratic failure criteria. The value of τ_{xz} is negligible in this analysis when compared to the matrix strength, allowing the Equation (3) to be simplified as

$$Fa_{out-of-plane} = \frac{\sigma_z}{Z_t} \qquad (4)$$

The out-of-plane strength in the z-direction (Z_t) is assumed to be the maximum calculated σ_z at the critical glass carbon interface at failure in the quasi-static test.

In the fatigue situation, changes in the residual through-thickness strength must be predicted. To do so, the failure criterion given in Equation (4) is assessed with the residual strength calculation approach outlined in Reifsnider (1996). Delamination is predicted to initiate when the residual strength calculated in this fashion is equal to the value of the failure criterion calculated using Equation (4).

Crack Growth

Following the onset of delamination, stiffness reduction of the compressive flange must also be considered with the tensile in-plane effects. These effects are also coupled with the crack growth and propagation to predict the ultimate failure of the beam. The reduction scheme is shown schematically in Figure 9. This stiffness reduction is used with the continued modulus reduction in the bottom (tensile) flange to determine the neutral axis shift. The new stiffness values and neutral axis location are then used to determine EI_{eff} and κ_x^o that allow for calculation of the stress state. The drop in stiffness and increase in curvature will inherently raise the stresses and may cause additional failures. The initial crack, and any newly formed cracks, are then monitored and continue through this evaluation cycle until failure. The process used to calculate the stiffness reduction in the compression flange, as well as the rate of delamination growth, is outlined below.

Compressive Flange Stiffness Reduction

The new modulus of the compression flange is determined through a rule of mixtures approach developed by O'Brien (1987)

$$E_x = (E^* - E_{lam})\frac{a}{b} + E_{lam} \qquad (5)$$

In Equation (5), a is the crack length of the largest crack in the laminate, b is the half width of the laminate, E* represents the effective modulus of the laminate if the layers are completely delaminated from each other, and E_{lam} is the initial effective modulus value of the laminate. The rule of mixtures is also used to determine E* :

$$E^* = \frac{\sum E_{x,i} t_i}{t} \qquad (6)$$

where $E_{x,i}$ and t_i represent the effective modulus and thickness of the sublaminates formed by the cracks.

Crack Growth

Once delamination initiates, crack growth is considered symmetric from each free edge of the beam. O'Brien has shown a good estimation of crack growth is based on the relation (O'Brien, 1987, 1993):

$$\frac{da}{dn} = \left(\frac{b}{E^* - E_{LAM}}\right)\left(\frac{dE}{dn}\right) \qquad (7)$$

dE/dn is the change in modulus over the step size, all other terms are consistent with their definitions above. The crack growth rate (da/dn) is not constant, since it is dependent on the number of layers that have delaminated at a given time, thus as more layers delaminate, the rate of crack growth increases.

Determining Failure of the Beam

The model predicts failure due to in-plane stresses (fiber failure) as well as out-of-plane stresses (delamination). Failure is assumed when either of the following criteria is met:

1. delamination initiates and the crack completely propagates across the width of the beam.
2. the in-plane remaining strength of the beam matches the loading (Fa = Fr).

Our experience has been that criterion 1, the out of plane stresses, control the strength and life of the beam. Confirmation of this will be shown in the results and discussion.

RESULTS AND DISCUSSION

Service Response of Tom's Creek Bridge

For replicate truck crossings for a given condition (lane and speed) the results of these calculations are tabulated in Tables 3 and 4 for strains and deflections. Only the last three load tests (fall 1998, spring 1999, and fall 1999) were used to calculate the dynamic load allowance based on deflection data. This is due to the fact that there were not enough deflectometers on the bridge to accurately depict the bridge's behavior during the first two load tests. For example, during fall 1999 there were six 40 mph (64 km/h) truck passes in the right lane. Using Table 3 it is seen that the maximum peak strain for those six runs was 409 με, while the average of the six peak values was 381 με. Table 4 shows that for the same test, in the same lane, the maximum peak deflection was 0.446 inches (11.3 mm), while the average of the six peak values was 0.415 inches (10.5 mm).

Results from the service load analysis of the Tom's Creek Bridge indicate that this composite structure underwent peak strains and deflections during the spring field tests. The maximum peak strain that a single girder experienced was 470 με during a 40 mph (64 km/h) left lane pass in spring 1998. The maximum peak deflection that a single girder underwent was 0.465 in (11.8 mm) during a 40 mph (64 km/h) right lane pass in fall 1998. The maximum

average peak strain for the bridge was 433 microstrain for 40 mph (64 km/h), left lane, truck passes in spring 1999. While the maximum average peak deflection was 0.430 in (10.9 mm) for 40 mph (64 km/h), right lane, truck passes in fall 1998. The bridge has a maximum average peak deflection of L/650, or 0.323 in (8.20 mm), for idle and 25 mph (40 km/h) truck crosses. However, the bridge has a maximum average peak deflection of L/490, or 0.430 in (10.7 mm), for 40 mph (64 km/h) truck crosses.

The AASHTO guidelines for the control of deflections for an all timber bridge is L/500 or 0.42 in in the AASHTO Standard Specification (AASHTO, 1996) and L/425 or 0.494 in in the AASHTO LRFD Specification (AASHTO, 1998). For a bridge with timber deck on steel girders the deflection is limited toL/800 or 0.263 in. in both specifications. Recall that there are no existing AASHTO design standards for a glulam deck on FRP composite girder bridge structure. These AASHTO guidelines are given because they represent the deflection control recommendations for typical small-span two lane bridges. The maximum measured deflection (L/490) was larger than that recommended by AASHTO for timber-steel bridges and approximately equal to that recommended for all timber bridges.

In general, idle and 25 mph (40 km/h) truck passes result in a similar bridge response with idle data being slightly higher than the 25 mph (40 km/h) values. The maximum bridge response always occurs during 40 mph (64 km/h) truck crosses, however, the location of this maximum varies between the right and left lanes. The maximum average peak strain for 40 mph (64 km/h) runs occurred in the left lane for all of the field tests with the exception of the fall 1998 test, when it occurred in the right lane. The maximum average peak deflection for 40 mph (64 km/h) runs occurred in the right lane for the fall 1998 and 1999 field tests and in the left lane for the spring 1999 field test. With only three test's worth of deflection data for analysis, it is impossible to predict if either lane results in the maximum deflection a majority of the time. One thing that is for certain, the maximum bridge response, whether strains or deflections, always occurs in either the right or left lane at 40 mph (64 km/h).

The data do not indicate any loss in stiffness of the bridge. Both the strains and the deflections that the bridge experienced during the first load test in fall 1997 are very similar in magnitude to the values obtained 2 years later during the fall 1999 field test.

Effect of Deck-to-Girder Connections on Bridge Stiffness

Service strains and deflections were determined for the "Tightened" afternoon runs in the same manner that the "As-Is" morning run values were calculated. In Tables 5 and 6, the average service load response has been compared for the "As-Is" and "Tightened" state and the percent change has been determined.

The expectation was that with the tightening of the Tom's Creek Bridge composite connections, the bridge will exhibit reduced service strains and deflections. However, Tables 5 and 6 show that the average peak strain and deflection values increased once the connections were tightened. The maximum average peak strain increased from 433 με to 454 με, albeit in the center lane as opposed to the left lane. The maximum average peak deflection increased from 0.415 in (10.5 mm) to 0.446 in (11.3 mm). For the right lane, the average strain value increased by approximately 15% for idle runs and 5% for 40 mph (64 km/h) runs. The left travel lane also

experienced an increase in strain of about 15% during idle runs. During 40 mph (64 km/h) truck crossings the left lane experienced a 4% reduction in strain for the spring 1999 field test but realized an increase in strain of 6% for the fall 1999 test. The center lane is where the increase in strain values are most dramatic. During idle runs the average center lane strain increase was 17% and 21% for 40 mph (64 km/h) runs. The results for deflection values are consistent with those for strain values. Again the only reduction in deflection values occurred during spring 1999 for the left lane at 40 mph (64 km/h). The deflection data verify that the load in the most heavily loaded girder actually increased when the deck-to-girder connections were tightened. Also, the deflection data reinforce the fact that the most dramatic increase in the response of the bridge's FRP composite girders, upon tightening of the connections, occurs when the truck crosses the center travel lane.

Tightening the connections seems to provide little in the way of composite action between the Tom's Creek Bridge's glue-laminated deck and FRP composite girders. During the composite bridge field testing, strains and deflections increased for identical truck crossings (lane and speed) as the day progressed. This increase is thought to be a function of the ambient air temperature, as the ambient air temperature increases, so to does the response (strains and deflections) of the FRP composite girders.

Dynamic Load Allowance

Typical composite girder midspan deflection during truck crossings is depicted in Figure 10. The figure presents the mid-span deflection for the most heavily loaded girder for a given truck crossing and are typical regardless of the truck's position on the bridge (right lane, center lane or left lane). In addition, the figure reveals the amplification of a quasi-static vehicular load once the vehicle becomes a moving load.

The measured IM values have been plotted as a function of time of service in Figures 11 and 12 where the average IM values are shown as well as current AASHTO standards for a glue-laminated deck on steel stringer bridge. Only the last three load tests were used to calculate the dynamic load allowance based on deflection data. This is due to the fact that there were not enough deflectometers on the bridge to accurately depict the bridge's behavior during the first two load tests. For design purposes a representative value for the entire bridge was desired. By including the center lane values, the IM was felt to underestimate the response of the bridge, particularly the left lane. It was discovered that the left and right side of the bridge demonstrated a greater dynamic response than the center lanes the source of which is unknown. As a result the IM results that follow are an average of right and left lane passes.

The speed of the truck as it approaches and crosses the bridge plays an important role in the magnitude of the dynamic load allowance. For the Tom's Creek Bridge there was little to no dynamic response when the truck crossed the bridge at 25 mph (40 km/h) as shown in the figures. However, when the truck crossed the bridge at 40 mph (64 km/h) the IM values ranged anywhere from as low as 0.2 (Figure 11) from strain data to 0.90 (Figure 12) from deflection data. The largest average value for IM shown in the two figures is 0.9 and is from deflection data. The results of this analysis are consistent with other tests that have been conducted in which the dynamic load allowance values both exceed AASHTO guidelines and display relatively large variations within the data (Billing, 1984).

Recommendations for IM for the Tom's Creek Bridge will be made based on deflection measurements. Deflection data are used over strain data for two reasons. First, strain gages do not accurately measure the total response of FRP composite girders. This is due to the fact that strain gages cannot detect shear deformations which can be significant with fiber-reinforced polymer composites. With a span of 17.5 ft (5.33 m), the shear deformation contribution to the FRP girders' response is approximately six percent of the total response. In addition, deflection data resulted in larger IM values and was therefore desirable, since it is extremely important to be conservative when designing with FRP composites. The strain data presented served as a validation for the results that are based on deflection data, therefore providing a necessary check on our results.

Transverse Wheel Load Distribution

The composite girders' behavior under typical heavy truck loading is shown in Figures 13 and 14. As expected the girders closest to the truck wheels carry most of the load.

Only the last three load tests were used to calculate the value of g based on deflection data for the same reasons as discussed earlier. Typically the center lane results yielded smaller distribution factors than the right or left lane passes, therefore, analysis of results will be based on the average of right or left lane truck crossings.

A summary of the design transverse wheel load distribution has been plotted as a function of time in Figures 15 and 16, where the current AASHTO standards for a glue-laminated deck on steel stringer bridge have been shown as well. In addition, the transverse wheel load distribution for an infinitely stiff bridge deck (effectively a lower bound on g) is shown. This value is equal to the number of lanes loaded, divided by the number of girders. In the case of the Tom's Creek Bridge, this value is equal to 1/24 or 0.042.

For the Tom's Creek Bridge, the difference between the maximum and minimum g values, for all of the load tests, at all three speeds, was only 0.016. No one speed consistently displayed the largest wheel load distribution values. The maximum Design g for the Tom's Creek Bridge is 0.101 or 10.1% of the total vehicle weight on the bridge (the rear tandem axle in this case). This value occurred during the fall 1998 field test as the truck crossed the bridge at 40 mph (64 km/h). With an average girder spacing, S, of 0.94 ft (0.29 m), this translates into a g value of S/9.3. Current AASHTO Standard Specification (AASHTO, 1996) requirements for a four inch thick glued laminated flooring on steel stringers are S/9.0 and S/8.0 (one and two design lanes loaded, respectively). The AASHTO LRFD Specification (AASHTO, 1998) values are S/8.8 and S/9.0 (one and two design lanes loaded, respectively) for a glulam deck on steel stringer bridge.

Based on the results from the Tom's Creek Bridge load tests, it is proposed that AASHTO design requirements for a glue-laminated deck on steel stringer bridge be adopted for the glue-laminated deck on FRP composite girder Tom's Creek Bridge. Deflection data were used as the primary source for wheel load distribution factor calculations because strain data do not measure the additional shear deformation that the FRP composite girders experience under load. Also, deflection data result in a slightly higher wheel load distribution factor, resulting in a

more conservative design. Although strain data have been presented, the purpose of these calculations was to validate our data that were based on deflection measurements. The inclusion of strain data provides a necessary check on our results.

Laboratory Results

Residual Stiffness Testing of FRP Composite Bridge Girders 1 and 2

The modulus of elasticity values in Table 7 are only for bending deformations since the mid-span shear is zero when a beam is subjected to four-point loading. In addition, the effective bending stiffness, or the product of the modulus and the moment of inertia, has been given. Finally, the P/δ value has been calculated for girders one and two. The reported P/δ number that is shown in Table 7 is the slope of the load versus deflection curve from 3 to 5 kips (the same loading region that was used to calculate the modulus). This value is a good indicator of the beams stiffness as it indicates the amount of load (kips) that it takes to deflect the composite girders one inch under four-point loading.

After 15 months of bridge service, girder one had a modulus value of 7080 ksi (48.8 GPa) while girder two has a modulus of 6900 ksi (47.6 GPa). This corresponds to a 1.25% decrease in the modulus of elasticity, and corresponding bending stiffness, for girder one and no change in the modulus, or the bending stiffness, for girder 2. The 1.25% decrease in modulus of elasticity is within experimental error. Under four-point loading it took 4.50 kips (20.0 kN) to deflect girder 1 one inch (25 mm) while it took 4.46 kips (19.8 kN) to deflect girder 2 one inch (25 mm). This makes sense since girder 1 is stiffer than girder 2 as is seen with the higher modulus value. After 15 months of service loading and one winter's worth of freeze-thaw cycles (51 as measured by on-site instrumentation) and deicing salts, the FRP composite girders have no significant loss in stiffness.

Residual Strength Testing of FRP Composite Bridge Girders 1 and 2

The data gathered from the strength tests performed on girders 1 and 2 are compared to ultimate strength data obtained from a different girder of the same batch that was tested prior to construction of the Tom's Creek Bridge. A summary of the ultimate strength values may be seen in Table 8.

Girder 1 failed at an ultimate load of 30.2 kips (134.3 kN). The mid-span deflection was 6.88 in (175 mm) and the top flange strain was 6530 με at failure. The mid-span bending moment in girder one was calculated to be 117 kip-feet (159 kN-m) at failure.

Girder 2, despite being less stiff than girder 1, failed at a significantly higher load of 35.7 kips (159 kN). The mid-span deflection was 8.37 in (213 mm) and the top flange strain was 8030 microstrain at failure. The mid-span bending moment in girder 2 was calculated to be 138 kip-feet (188 kN-m) at failure.

The FRP composite girders suffered a sudden, explosive failure that was the result of delamination of the compression (top) flange, while the tensile flange remained intact. Figure 8 shows one of the FRP composite girders after experiencing such a failure. This failure is best

represented in Figure 17 where load versus strain and deflection has been plotted up to failure. Strains and deflections increase linearly until failure at which time the composite girders lose the ability to carry load. Both girder 1 and girder 2 displayed larger values for failure load and top flange failure strain when compared to a similar Batch 1 beam that was failed prior to construction of the Tom's Creek Bridge. Girder 1 displayed a 3.4% increase in failure load while girder 2 failed at a load that was 22.3% greater than the 29.2 kips (130 kN) that the similar Batch 1 beam failed at. Based on comparisons to a similar beam from the same batch it appears that there has been little, if any, change in the ultimate strength of the FRP composite bridge girders.

Fatigue Life Prediction Compared to Experimental

The stiffness reduction for a girder fatigued at 53% of the ultimate moment capacity is shown experimentally and that predicted from the theoretical analysis in Figure 18. Observe that both the top and bottom flanges lose about 2% of their stiffness over the nearly 40,000 cycles. The stiffness reduction in the tensile flange is based solely on coupon data. As expected a reduction in compression flange stiffness is not predicted. Still the model does a reasonable job at modeling the stiffness reduction for the overall beam and can be used by designers to suggest the loss in stiffness of a bridge as a result of fatigue. The sudden loss of stiffness at the end of life is indicative of the propagation of the delamination across the width of the flange.

In terms of failure for all cases investigated delamination is predicted as the primary failure mode, shown in Figure 19. This is noted when the remaining strength (delamination strength) is exceeded by the out of plane stress state, inducing delamination. Note that the stress required for in-plane failure of the laminates of the girder is more than four times higher than the stress required to cause out-of-plane failure.

An S-N curve was created for the beam considering no neutral axis shift and using the overall average ultimate moment data to determine the strength of the beam. The experimental points and the predicted S-N curve are shown in Figure 20, normalized to the average ultimate moment of all the hybrid beams tested from both batches. The beam failure at 53% is about 7 orders of magnitude from the prediction. The two beams which experienced runout at 8 and 10 million cycles were under the predicted failure. The beam that failed after 370,000 cycles at 71% of the average ultimate moment agrees well with the prediction of 300,000 cycles at the same load. Without further data, the validity of the model overall cannot be determined.

What is important to note from this analysis is that the Tom's Creek Bridge service moment is less that 10% of the ultimate moment capacity for the DWB. The analysis suggests that fatigue will not be a concern over the life of the bride considering the light traffic volume and loads. However, the environmental effects have not as yet been included in this analysis and will contribute to stiffness loss that will reduce the life of the girder by increasing the stress needed to cause delamination.

CONCLUSIONS

As a result of research conducted on the FRP composite Tom's Creek Bridge, the following conclusions are made:

- For the FRP composite Tom's Creek Bridge, the maximum service deflection response has been determined to be 0.430 in (11 mm). This corresponds to a service deflection of L/490, where L is the clear-span length. This value is consistent with AASHTO deflection control criteria for an all timber bridge of L/425 (LRFD Specification) and L/500 (Standard Specification). However, the service deflections for the Tom's Creek Bridge greatly exceed the recommendations for a timber deck on steel girder bridge of L/800.

- There is little, if any, dynamic amplification of an applied load on the bridge due to a vehicle moving at 25 mph (40 km/h). However, at 40 mph (64 km/h) the composite bridge exhibits a relatively large dynamic response.

- The transverse wheel load distribution factor, g, for the bridge's composite girders has been determined. The wheel load distribution factor is not a function of the vehicle's speed and although typical for the right and left lane loading, is smaller for the center lane loading. The decrease in the center lane g value is due to the fact that a center lane load is effectively distributed to a larger number of bridge girders. For the Tom's Creek Bridge, a distribution factor of 0.101, or 10.1%, has been calculated. For the Tom's Creek Bridge, a g value of 0.101 is the equivalent of S/9.3, where S is the average girder spacing in feet. The calculated distribution factor is conservatively less than the AASHTO requirements (both LRFD and the Standard Specification) for a glulam timber deck on steel stringer bridge.

- The effect of the Tom's Creek Bridge's deck-to-girder connections was investigated. By comparing data gathered immediately after tightening of the connections to data collected prior to tightening of the connections it has been determined that the composite connections do not contribute significant additional stiffness to the bridge.

- Bridge girders 1 and 2 were removed after 15 months of service and tested for stiffness and strength. These data were compared to stiffness and ultimate strength values established prior to the construction of the bridge. After 15 months, there was no apparent loss in the stiffness of the girders. Likewise, the ultimate strength of each FRP girder, 30.2 kips (134 kN) for Girder 1 and 35.7 kips (159 kN) for Girder 2, is consistent with the pre-service data, indicating no apparent losses, after 15 months of service, in the ultimate strength of the FRP composite beams.

- A life prediction methodology is developed and experimentally investigated for four point bending fatigue of the DWB girder. This analysis relies on the coupon data to suggest the fatigue performance of the girder. Comparisons with experimental results show that the stiffness reduction can be predicted with reasonable accuracy. However there is insufficient fatigue failure data to validate the model in predicting fatigue life.

- The fatigue life model, although not fully validated, does suggest that designers can use the stiffness reduction information to assess the loss in stiffness of the girder (and ultimately the

bridge) based on fatigue. For the case of a girder fatigued at 53% of the ultimate moment capacity, only a 2% reduction in bending stiffness was observed.

- Given the low service loads (no more than 10% of the ultimate capacity) and traffic volume the model suggests that fatigue will not be a major concern during the life of service (10-15 years).

RECOMMENDATIONS

1. A dynamic load allowance, IM, of 0.90 is recommended for the Tom's Creek Bridge. This value is the largest average IM observed and is therefore conservative. This value is significantly higher than those set forth in the AASHTO standards of 0.33 (AASHTO, 1998) and 0.30 (AASHTO, 1996).

2. It is recommended to use a value of L/425 (LRFD Specification) or L/500 (Standard Specification). This value is consistent with AASHTO deflection control criteria for an all timber bridge.

3. It is recommended to use the AASHTO wheel load distribution factors for a glulam timber deck on steel stringer bridge.

4. Tests conducted on the long-term performance of the FRP composite bridge girders were conducted after only 15 months of service. To be able to predict long-term losses better in stiffness with a greater degree of confidence the girders should be tested periodically for stiffness values. In one day, two girders can be removed, tested for stiffness and then placed back in the bridge. In addition, when the Tom's Creek Road is widened in approximately 5 years, girders from each batch (Batch 1 and Batch 2) should be tested to failure. This would indicate if exposure to bridge service conditions over a period of 10 years results in a loss in the ultimate strength of the FRP composite girders.

REFERENCES

AASHTO (1998). *LRFD Bridge Design Specification,* 2nd ed., American Association of State Highway and Transportation Officials, Washington, D.C.

AASHTO (1996). *Standard Specification for Highway Bridges,* 16th ed., American Association of State Highway and Transportation Officials, Washington, DC.

Billing, J.R. (1984). Dynamic Loading and Testing of Bridges in Ontario, *Canadian Journal of Civil Engineering,* Vol. 11, pp. 833-843.

Brewer, J.C. and Lagace, P.A. (1988). Quadratic Stress Criterion for Initiation of Delamination, *Journal of Composite Materials,* Vol. 22, December, pp. 1141-1155.

Hayes, M.D., J.J. Lesko, J. Haramis, T.E. Cousins, J. Gomez, and P. Masarelli (2000). Laboratory and Field Testing of a Composite Bridge Superstructure, *Journal of Composite Construction,* ASCE, Vol. 4, No.3, August 2000, pp. 1-9.

Hayes, M.D. (1998). *Characterization and Modeling of a Fiber-Reinforced Polymeric Composite Structural Beam and Bridge Structure for Use in the Tom's Creek Bridge Rehabilitation Project,* M.S. Thesis, Dept of Engineering Science & Mechanics, Virginia Polytechnic Institute & State University, Blacksburg.

Hwang, E.S. and A.S. Nowak (1990). Dynamic Analysis of Girder Bridges, *Transportation Research Record 1223,* Transportation Research Board, Washington, D.C., pp. 85-92.

Hyer, M.W. (1998). *Stress Analysis of Fiber-Reinforced Composite Materials,* WCB/ McGraw-Hill, New York, NY, p. 606.

Neely,W.D. (2000). *Evaluation of the In-Service Performance of the Tom's Creek Bridge,* M.S. Thesis, Virginia Polytechnic Institute & State University, Blacksburg.

O'Brien, T.K. (1987). Generic Aspects of Delamination in Fatigue of Composite Materials, *Journal of the American Helicopter Society*, Vol. 32, January, pp. 13-18.

O'Brien, T.K. (1993). Stacking Sequence Effect on Local Delamination Onset in Fatigue, International Conference on Advanced Composite Materials, *The Minerals, Metals & Materials Society,* pp. 399-406.

Phifer, S.P. (1999). *Quasi-Static and Fatigue Evaluation of Pultruded Vinyl Ester/E-Glass Composites,* M.S. Thesis, Dept of Engineering Science & Mechanics, Virginia Polytechnic Institute & State University.

Reifsnider, K. L., Iyengar, N., Case, S. W. and Xu, Y. L. (1996). *Damage Tolerance and Durability of Fibrous Material Systems: A Micro-Kinetic Approach, Durability Analysis of Structural Composite Systems,* A. H. Cardon (ed). A. A. Balkema (Rotterdam), 123-144.

Senne, J.L. (2000a). *Fatigue Life of Hybrid FRP Composite Beams,* M.S. Thesis, Department of Engineering Science & Mechanics, Virginia Polytechnic Institute & State University, Blacksburg.

Senne, J., Lesko, J. J., and Case, S. W. (2000b). A Life Prediction Methodology for Thick Section Composites Used in Civil Infrastructure, *ASTM Journal of Composite Science & Technology,* Vol. 22, No. 4, October, pp. 241-248.

Strongwell (2000). Extren DWB^{TM} Design Guide, Strongwell Corporation, Bristol, VA.

Table 1. Section properties for the 8 inch FRP composite beams.

8" FRP Beam Properties	English Units	SI Units
Area	13.7 in^2	88.4 cm^2
Depth	8.0 in	20.3 cm
Outer Width of Web Box	3.0 in	7.62 cm
Web Thickness	0.36 to 0.42 in	0.91 to 1.07 cm
Flange Width	6.0 in	15.2 cm
Flange Thickness	0.62 in	1.57 cm
Moments of Inertia	I_{xx} – 129 in^4 I_{yy} = 31.7 in^4	I_{xx} – 5350 cm^4 I_{yy} = 1320 cm^4

Table 2. Fatigue test conditions for each beam.

	Max Actuator Load (lbs)	Min Actuator Load (lbs)	R-Ratio (Min/Max)	Frequency (Hz)
Beam 425	16,000	1720	0.11	0.85
Beam 421	20,100	1300	0.06	0.60
Beam 514	20,010	2700	0.13	0.82
Beam 517	27,085	7500	0.28	0.70

Table 3. Service load strains (με) recorded during the Tom's Creek Bridge field tests.

Test Date	Speed (mph)	Truck Position								
		Right Lane			Left Lane			Center Lane		
		No. of Passes	Max Peak Strain	Avg Peak Strain	No. of Passes	Max Peak Strain	Avg Peak Strain	No. of Passes	Max Peak Strain	Avg Peak Strain
Fall 1997	Idle	2	271	268	2	235	232	2	230	229
	25	2	266	255	2	227	214	3	219	214
	40	2	358	356	2	419	383	2	374	343
Spring 1998	Idle	4	323	300	4	290	275	4	321	316
	25	3	318	299	3	310	300	4	317	299
	40	4	369	314	4	470	383	4	407	353
Fall 1998	Idle	5	259	255	6	218	213	6	222	213
	25	4	284	268	5	248	239	7	223	206
	40	5	428	393	4	373	367	5	311	272
Spring 1999	Idle	6	303	297	6	280	262	6	331	324
	25	3	299	285	3	274	268	6	310	290
	40	4	449	419	4	447	433	6	432	376
Fall 1999	Idle	6	285	265	6	246	235	5	253	219
	25	3	245	231	3	230	224	3	202	197
	40	6	409	381	5	396	385	5	317	272

Table 4. Service load deflections (inches) recorded during the Tom's Creek Bridge field tests. Note that AASHTO deflection control recommendations for a bridge with this span are: Timber & Steel Bridge = 0.263 in, All Timber Bridge (Standard Spec.) = 0.420 in and All Timber Bridge (LRFD Spec.) = 0.494 in.

Test Date	Speed (mph)	Truck Position								
		Right Lane			Left Lane			Center Lane		
		No. of Passes	Max Peak Defl. (in)	Avg Peak Defl. (in)	No. of Passes	Max Peak Defl. (in)	Avg Peak Defl. (in)	No. of Passes	Max Peak Defl. (in)	Avg Peak Defl. (in)
Fall 1998	Idle	5	0.261	0.252	6	0.188	0.179	6	0.213	0.208
	25	4	0.304	0.271	5	0.203	0.196	7	0.206	0.195
	40	5	0.465	0.430	4	0.381	0.372	5	0.288	0.257
Spring 1999	Idle	6	0.280	0.272	6	0.241	0.226	6	0.327	0.323
	25	3	0.277	0.264	3	0.227	0.223	6	0.276	0.259
	40	4	0.410	0.384	4	0.413	0.394	6	0.415	0.357
Fall 1999	Idle	6	0.322	0.262	6	0.200	0.181	5	0.229	0.184
	25	3	0.262	0.233	3	0.191	0.183	3	0.173	0.169
	40	6	0.446	0.415	5	0.378	0.360	5	0.300	0.247

Table 5. Change in service strains (με) after tightening of the Tom's Creek Bridge deck-to-girder connections.

Test Date	Speed (mph)	Truck Position								
		Right Lane			Left Lane			Center Lane		
		As-Is Average	Composite Average	% Change	As-Is Average	Composite Average	% Change	As-Is Average	Composite Average	% Change
Spring 1999	Idle	297	335	+13	262	303	+16	324	348	+ 7
	40	419	436	+ 4	433	415	- 4	376	454	+ 21
Fall 1999	Idle	265	301	+ 14	235	261	+ 11	219	275	+ 26
	40	381	401	+ 5	385	407	+ 6	272	327	+ 20

Table 6. Change in service deflections (inches) after tightening of the Tom's Creek Bridge deck-to-girder connections.

Test Date	Speed (mph)	Truck Position								
		Right Lane			Left Lane			Center Lane		
		As-Is Average	Composite Average	% Change	As-Is Average	Composite Average	% Change	As-Is Average	Composite Average	% Change
Spring 1999	Idle	0.272	0.306	+ 13	0.226	0.277	+ 23	0.323	0.354	+ 10
	40	0.384	0.427	+ 11	0.394	0.377	- 4	0.357	0.440	+ 23
Fall 1999	Idle	0.262	0.278	+ 6	0.181	0.223	+ 23	0.184	0.261	+ 42
	40	0.415	0.446	+ 7	0.360	0.374	+ 4	0.247	0.289	+ 17

Table 7. Stiffness values for the FRP composite Tom's Creek Bridge girders 1 and 2. Data are shown for both girders prior to the bridge's construction and then after 15 months of service.

Stiffness Parameter	Bridge Girder 1		Bridge Girder 2	
	Pre-Service	Post-Service	Pre-Service	Post-Service
Young's Modulus of Elasticity, E (ksi)	7,170	7,080	6,900	6,900
Bending Stiffness, EI (kips-inches^2)	922,000	910,000	887,000	887,000
Load vs. Deflection, P/δ (kips/inch)	--------	4.50	--------	4.46

Table 8. Ultimate strength values for the FRP composite Tom's Creek Bridge girders 1 and 2. Data are shown for girders 1 and 2 after 15 months of service. *Pre-service data are taken from a beam that was failed prior to construction of the Tom's Creek Bridge that was from the same batch (Batch 1) as girders 1 and 2.

Strength Parameter	Bridge Girder 1		Bridge Girder 2	
	Pre-Service	Post-Service	Pre-Service	Post-Service
Top Flange Failure Strain, με (microstrain)	6,210*	6,530	6,210*	8,030
Mid-Span Failure Deflection, δ (inches)	--------	6.88	--------	8.37
Failure Load, P (kips)	29.2*	30.2	29.2*	35.7
Failure Moment, M (kip-feet)	113*	117	113*	138

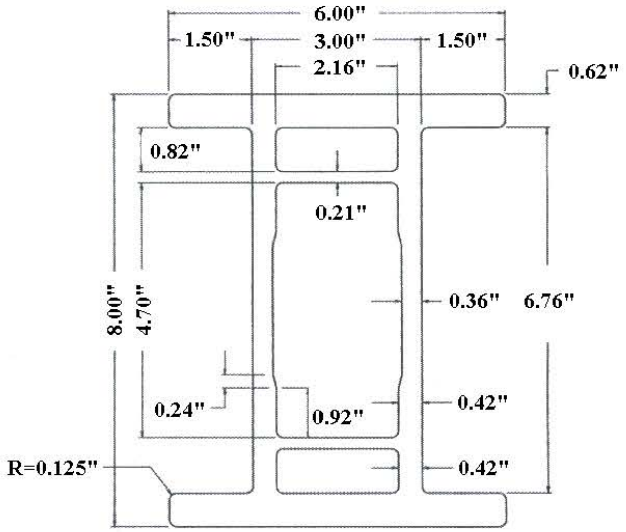

Figure 1. Cross-section of the 8-in fiber-reinforced polymer composite beams used in the Tom's Creek Bridge rehabilitation.

Figure 2. The completed Tom's Creek Bridge.

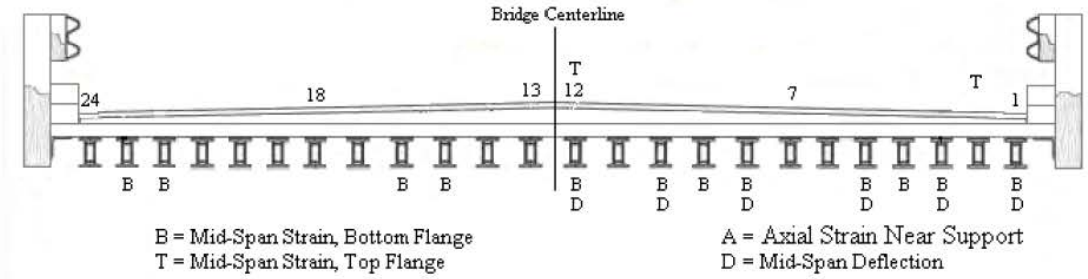

a) Initial instrumentation plan

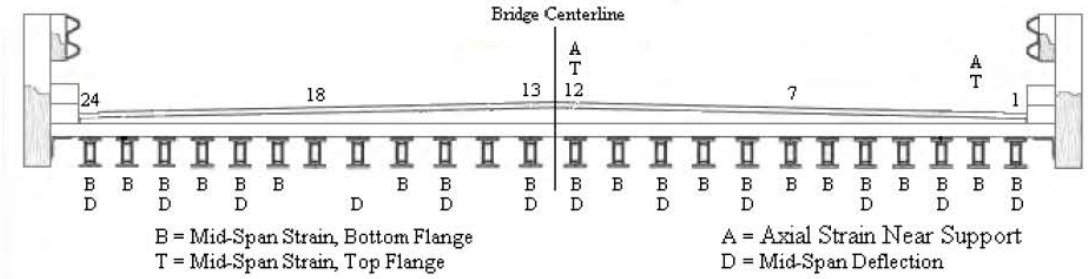

b) Final instrumentation plan

Figure 3. Instrumentation plan evolution.

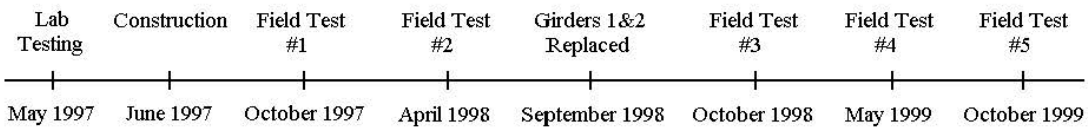

Figure 4. Timeline detailing the history of the Tom's Creek Bridge.

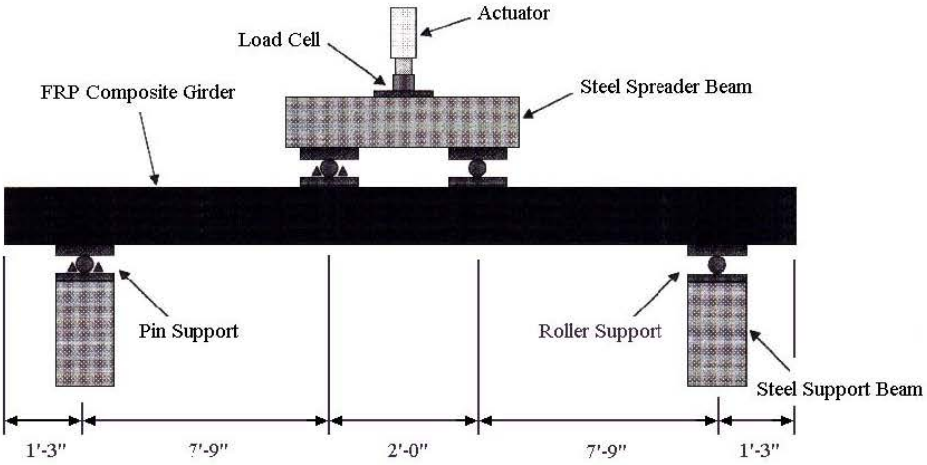

Figure 5. Schematic of four-point strength and stiffness setup.

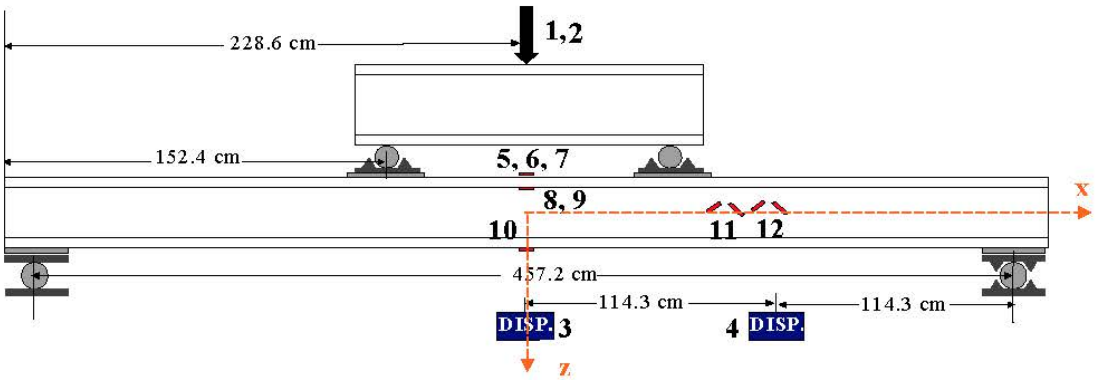

Figure 6. Schematic for the instrumentation used in the characterization of strength and fatigue. 1. Actuator Load, 2. Actuator deflection, 3. Mid-span Deflection, 4. Quarter Point Deflection, 5. Top Center Bending Strain, 6. Top Right Bending Strain, 7. Top Left Bending Strain, 8. Top Right Flange Bending Strain, 9. Top Left Flange Bending Strain, 10. Bottom Center Bending Strain, 11. Shear Strain 1 in outside of the constant moment region, 12. Torsional Strain at the ¼ point.

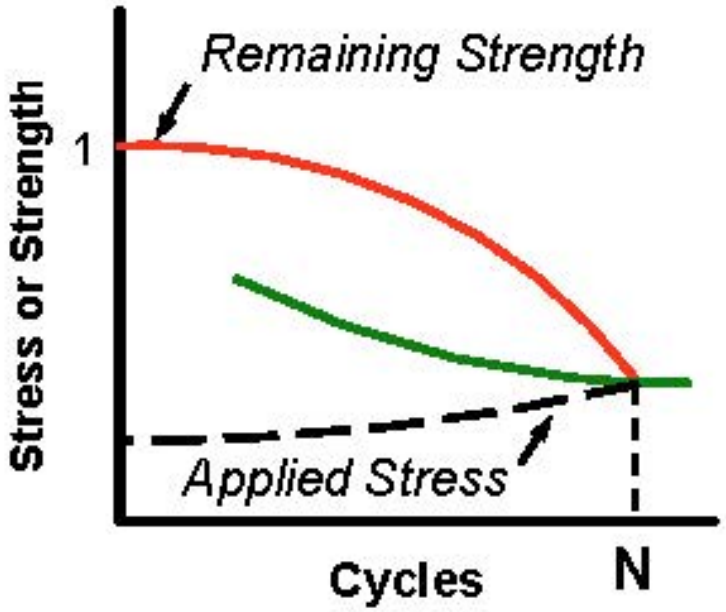

Figure 7. The use of remaining strength as a damage metric.

Figure 8. Failure of the compression flange for removed Tom's Creek Bridge FRP composite Girder 1. Note failure occurs at mid-span.

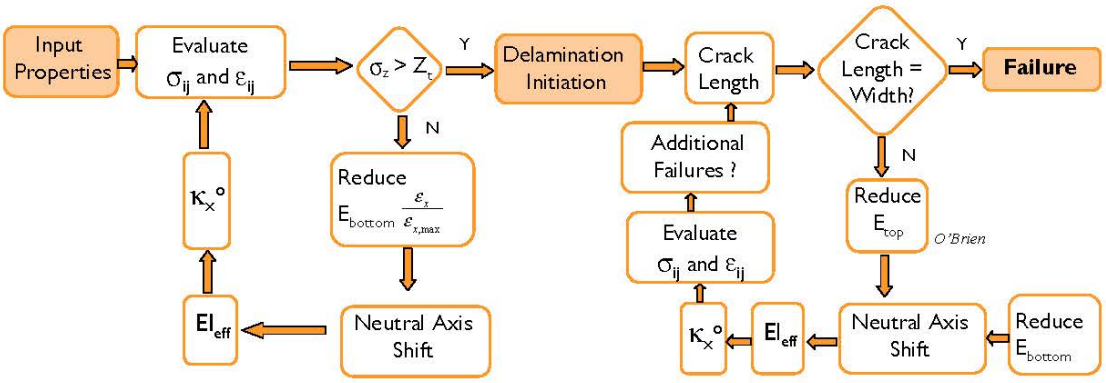

Figure 9. Flowchart of stress analysis and stiffness reduction, delamination determination, and stress redistribution following delamination.

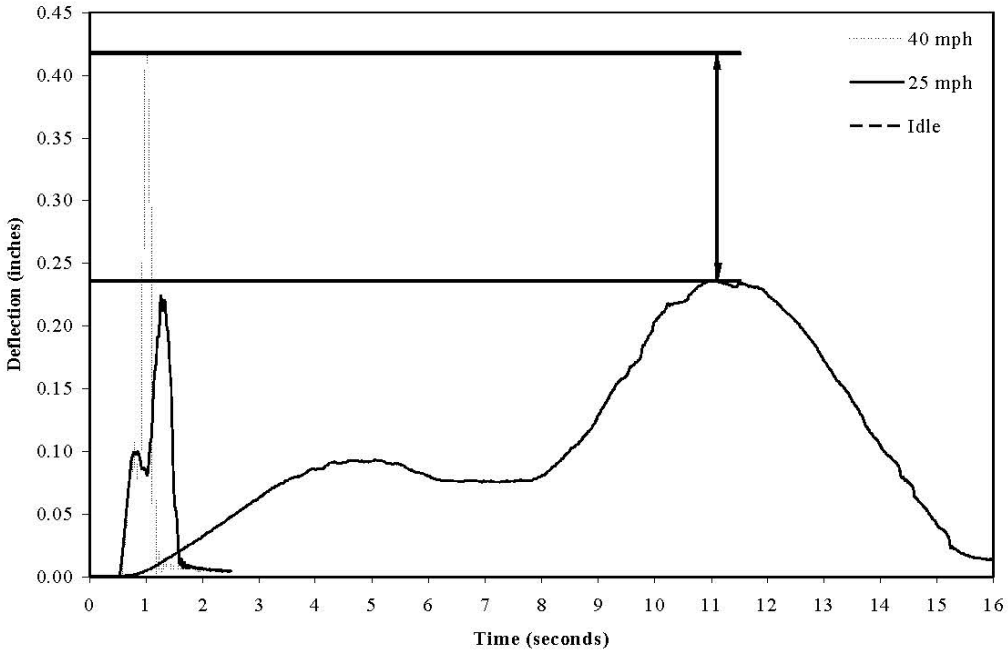

Figure 10. Typical Tom's Creek Bridge composite girder response (mid-span deflections) due to heavy truck loading.

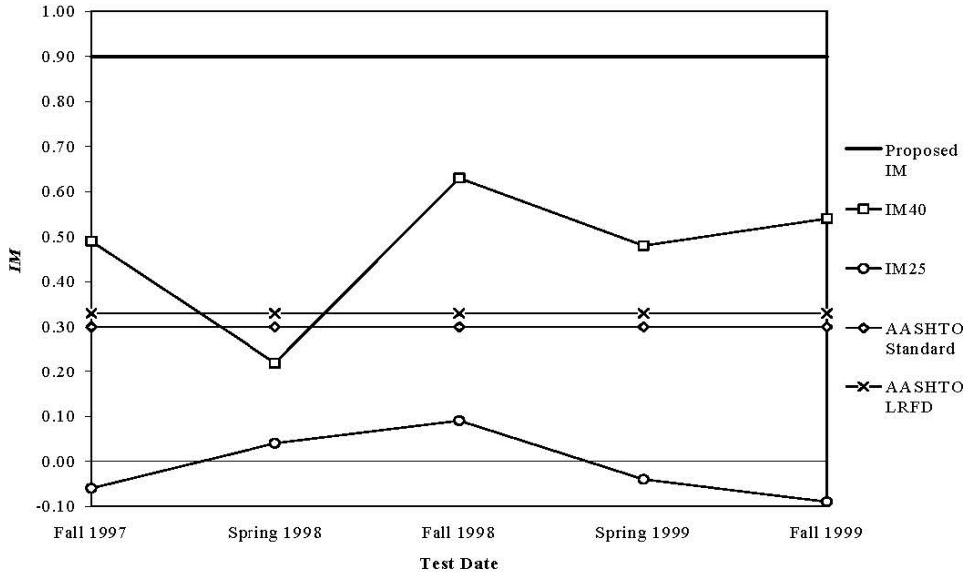

Figure 11. IM values based on mid-span strain data.

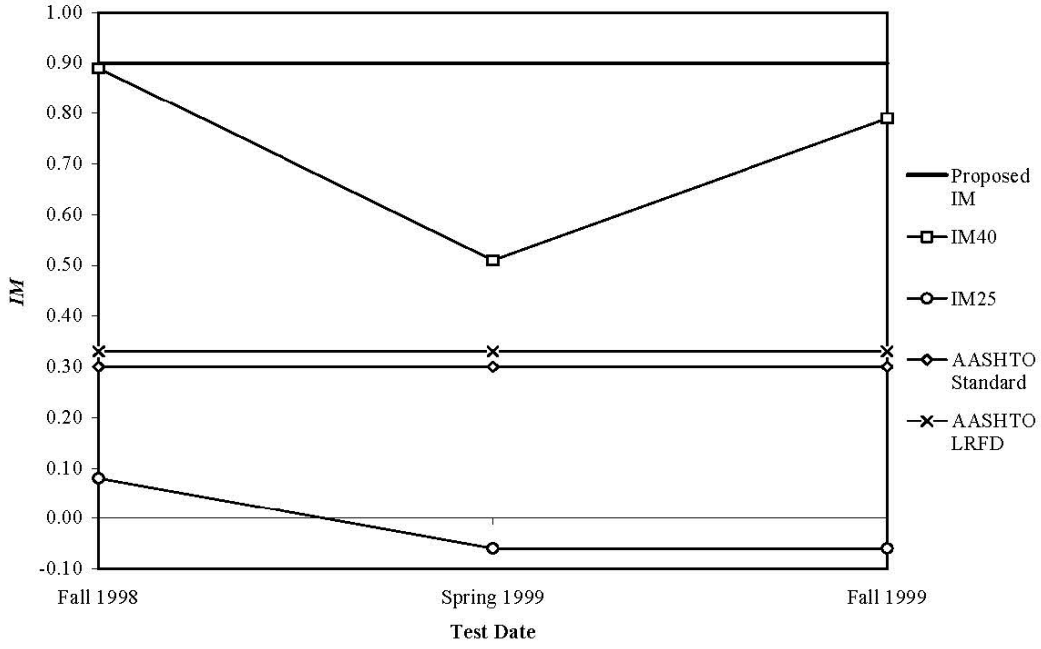

Figure 12. IM values based on mid-span deflection data.

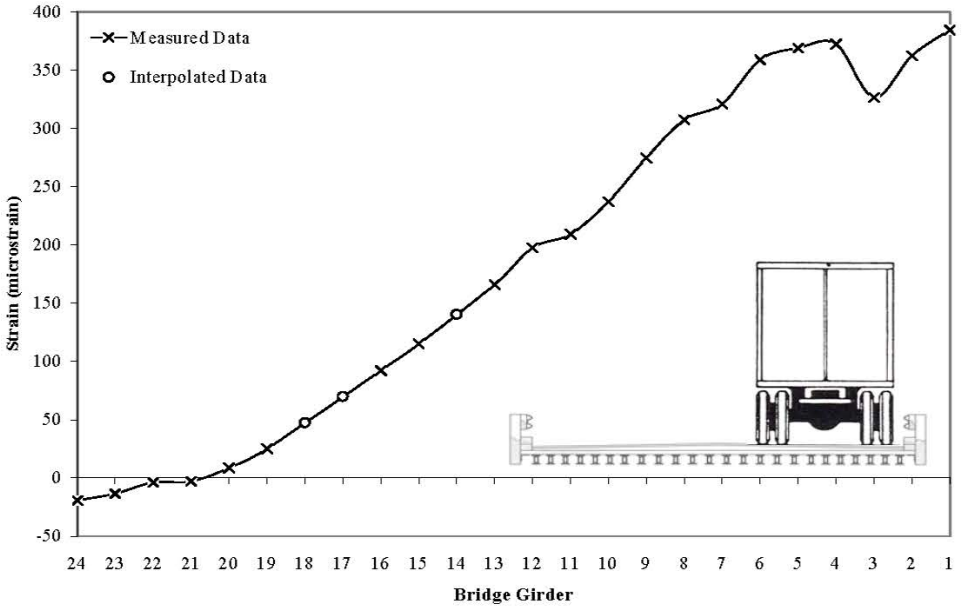

Figure 13. Typical Tom's Creek Bridge composite girder response under heavy truck crossing, right lane 40 mph.

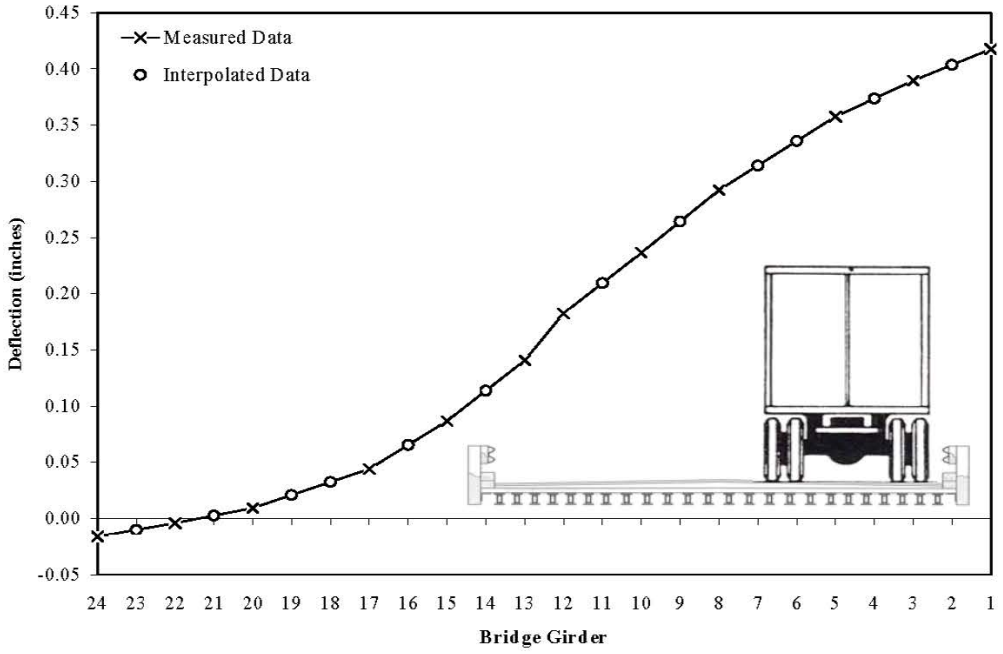

Figure 14. Typical Tom's Creek Bridge composite girder response under heavy truck crossing, right lane 40 mph.

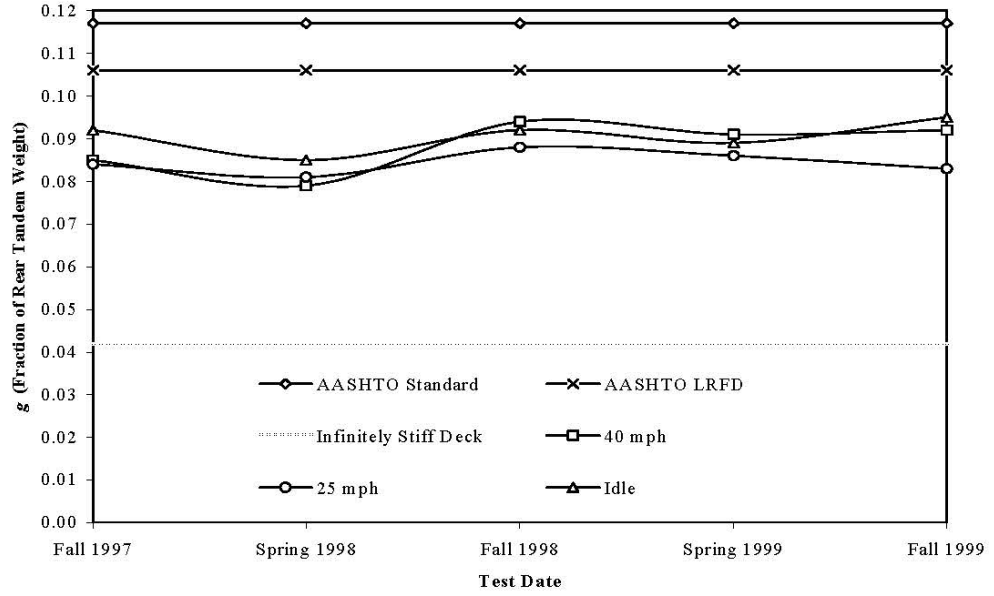

Figure 15. Summary of the design wheel load distribution factor, g. Values based on mid-span strain data.

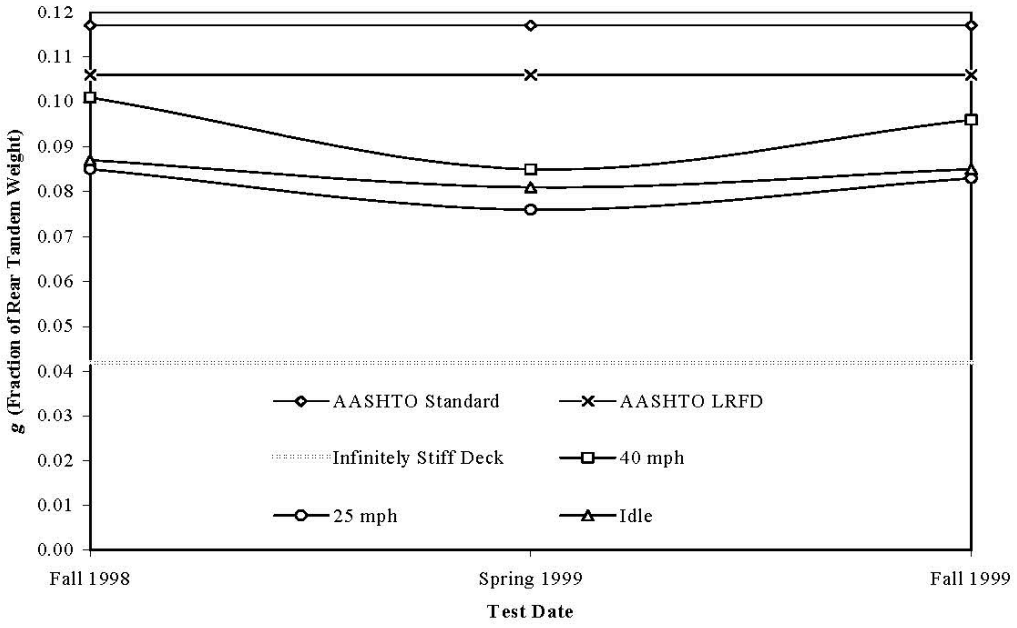

Figure 16. Summary of the design wheel load distribution factor, g. Values based on mid-span deflection data.

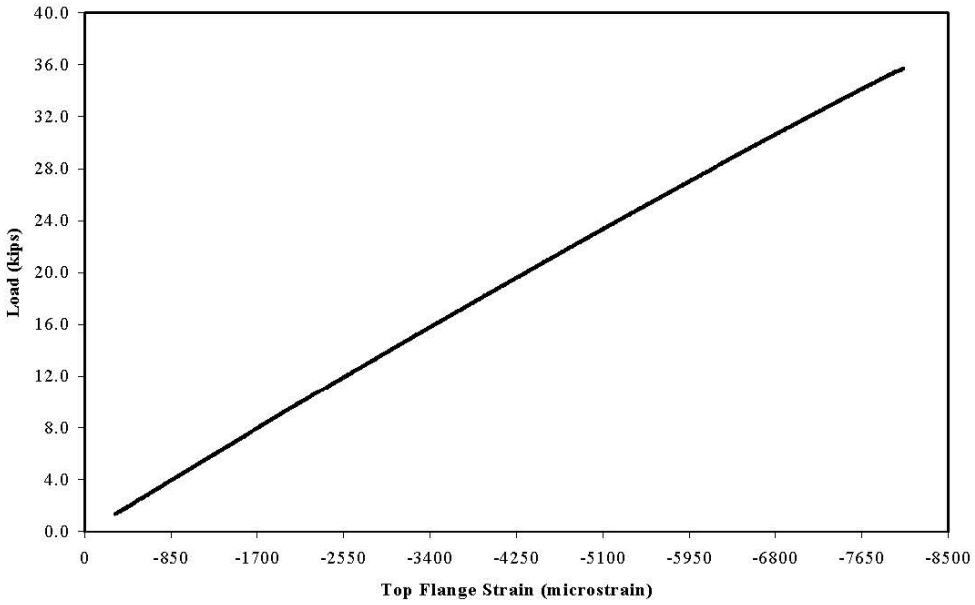

Figure 17. Load versus top flange strain to failure for FRP composite girder 2, failed after fifteen months of service in the Tom's Creek Bridge.

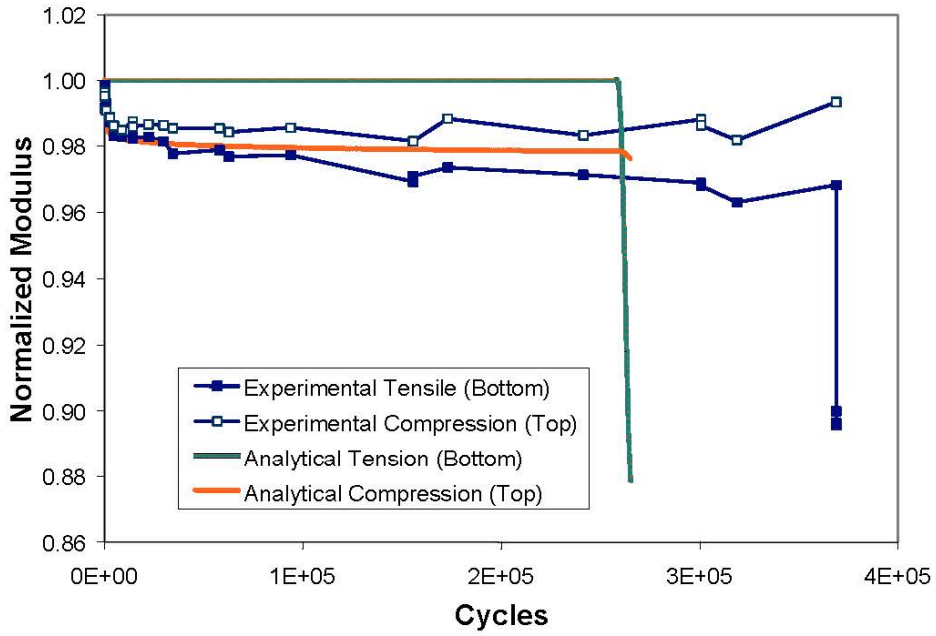

Figure 18. Stiffness reduction (predicted and measured) curve for the girder fatigued at 53% of the ultimate moment capacity.

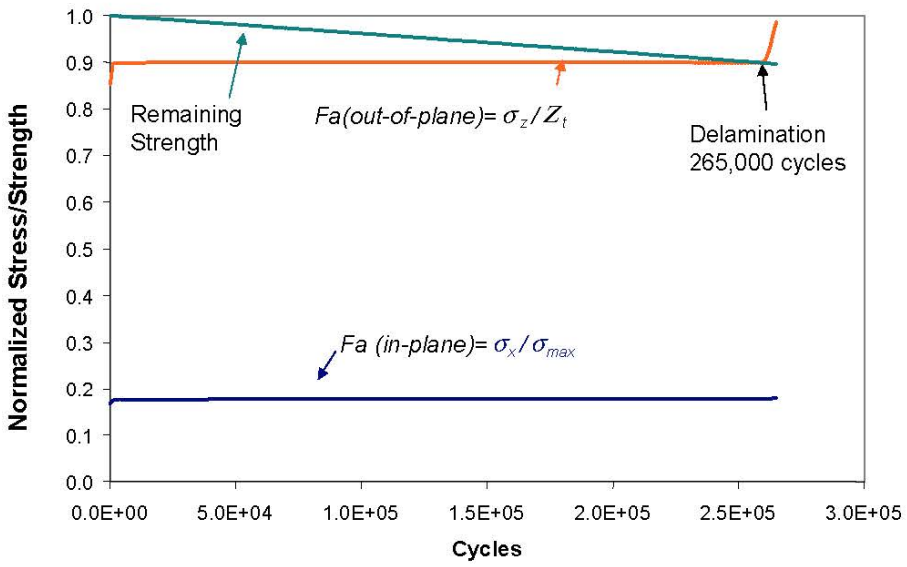

Figure 19. Graphical representation of remaining strength and the stress on the critical element. This analysis is shown for an applied moment, 85% of the ultimate moment capacity.

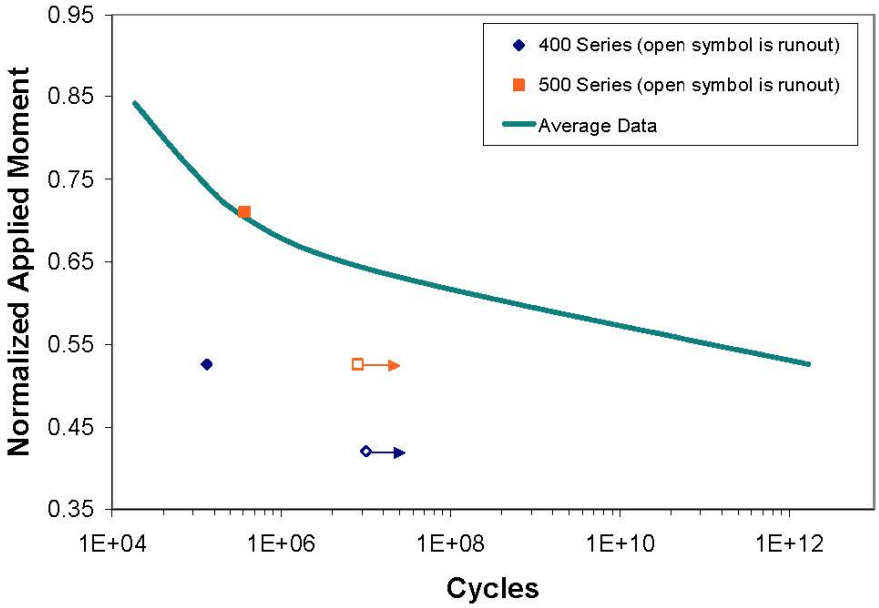

Figure 20. Comparison of predicted S-N curve for beam fatigue loading to experimental data. The 400 and 500 series beams are designations of different processing runs.